International Journal of Research in Engineering and Science (IJRES)
ISSN (Online): 2320-9364, ISSN (Print): 2320-9356
www.ijres.org Volume 12 Issue 5 ǁ May 2024 ǁ PP. 203-207

Analyze the amplitude of the ultrasonic transducer using the finite element method

Hoang Anh Quang, Ha Bach Tu*
Faculty of Mechanical Engineering, Thai Nguyen University of Technology, Thai Nguyen, Viet Nam
Corresponding Author: Ha Bach Tu

Abstract
A transducer is a device that plays a very important role in the ultrasonic vibration system. It has the function of converting electrical energy into mechanical energy. Today, the process of optimal design of this device has been aided by computers through finite element analysis software. In this study, a finite element model of the transducer is built to study the effect of meshing on the vibration amplitude of the transducer. The results show that the mesh size of the element in the FEM model has an influence on the vibration amplitude at the resonant frequency of the transducer. The research results are the basis for expanding related research in the field of ultrasonic vibration.

Keywords: *transducer, mesh size, finite element, simulation*

Date of Submission: 06-05-2024 Date of acceptance: 18-05-2024

I. INTRODUCTION

Ultrasonic vibration is applied in many different fields such as modern medicine and medical diagnosis, chemical and food processing, metal joining and machining, etc. In addition, ultrasonic vibration is also used in fields that require high sensitivity such as maritime, safety and defense sector. During material processing, ultrasonic vibrations reduce energy consumption and process costs. In these different fields, the purpose of ultrasonic vibration application is either primary or secondary. The main purpose of ultrasound application involves the fields of medical diagnosis, food processing, and ultrasonic welding, etc. where ultrasonic vibration plays a major role in the finishing process. The secondary purpose involves applying ultrasonic vibration to aid the process to improve process efficiency. The application of ultrasonic vibrations in metalworking has been around since the first decades of the 20th century. Various manufacturing processes such as machining, forming, joining, etc. assisted by ultrasonic vibration to improve the properties of the finished product. These ultrasonic vibrations themselves are physical vibrations of molecules in the medium through which the sound is transmitting. The frequency range from ∼20 kHz to several GHz is often referred to as the ultrasonic range. The effects of ultrasonic vibrations on metals and alloys are mainly used for manufacturing purposes. The results of the integration of ultrasonic in metal processing are fully available in the literature [1–8] The effects of ultrasonic energy are similar to using heat to soften materials; however, experimental results show that the ultrasonic energy required to produce the same amount of softening is 107 times smaller than the thermal energy required. Some researchers in their research have used ultrasonic vibrations to metal working and the results show that the force required for machining is significantly reduced compared to the force used in other conventional pressure machining method. Nowadays, ultrasonic metal machining is increasingly widely used because it has a number of advantages such as: The ultrasonic process is clean, reliable, consistent and affordable; Does not use any consumables and is user and environmental friendly, fast and repeatable; Utrasonic eliminates subjective factors in the welding process, ensuring stable quality; Low energy consumption; Setup is quick and easy. The versatility of the ultrasonic method allows changing from one setting to another within minutes; The tool has a long life and requires little or no maintenance [9]. It is also known as green technology for the reason that it can be applied to many processes without harming the environment or humans. With these advantages, ultrasonic method is being applied more and more widely in many fields. For effective application, studying the characteristics of ultrasonic vibration is essential. The finite element method is a useful tool in these studies. In study of D. A. DeAngelis et al, the finite element method was used to check the selection of loading bolts when designing Langevin type transducers [10]. In addition, many studies also use the finite element method to calculate and analyze ultrasonic vibration equipment and systems [11,12]. However, the effect of element mesh size on vibration amplitude has not been mentioned. In this study, the effect of element size on longitudinal vibration amplitude of the transducer will be carried out.

II. THEORETICAL ANALYSIS

Based on studies on ultrasonic vibrating heads [13–15], a transducer model was selected for research (Figure 1). The transducer works at a resonant frequency of 20 kHz and a longitudinal oscillation amplitude of 10 µm. Component sizes and material specifications are given in Table 1 and Table 2.

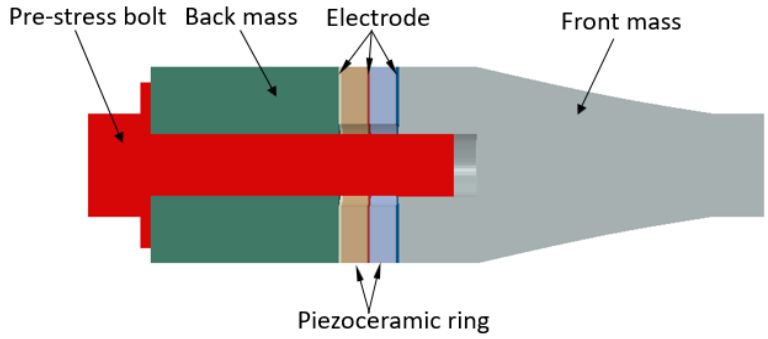

Figure 1: Components of an ultrasonic transducer

Table 1: The dimensions of ultrasonic transducer parts

Component	External diameter (mm)	Bore size (mm)	Length (mm)	Material
Back mass	38	12	36	Steel
Piezoelectric ceramic ring	38	16	8	PZT4
Pre-stress bolt	12		60	Titanium
Electrode sheet	38	16	0.5	Copper
Front mass (Cylindrical segment 1)	38	12	15	Titanium
Front mass (Conical segment)			45	Titanium
Front mass (Cylindrical segment 2)	20		10	Titanium

Table 2: *Material parameters*

Material	Density ($kg.m^{-3}$)	Elastic modulus (GPa)	Poisson ratio
PZT-4	7600	65	0.31
Copper	8900	115	0.31
Titanium	4418	110	0.34
Steel	7800	209	0.3

In the structure of the transducer, the ceramic ring plays a very important role in converting electrical energy into mechanical energy. Therefore, it is necessary to accurately calculate the values that need to be provided to the FEM model. The basis for calculating the parameters of ceramic materials is as follows:

Linear electrical behavior of ceramic materials:

$$D = \varepsilon E \Rightarrow D_i = \varepsilon_{ij} E_j \tag{1}$$

D is the electric charge density displacement, ε is permittivity, and E is electric field strength. The Hooke's law for elastic materials:

$$S = sT \Rightarrow S_{ij} = s_{ijkl} T_{kl} \tag{2}$$

Where, S is strain, s is compliance under short-circuit conditions T is stress. These relations may be combined into so-called coupled equations, of which the strain-charge form is:

$$\begin{aligned} S &= sT + d^t E \\ D &= dT + \varepsilon E \end{aligned} \tag{3}$$

Where d is the matrix for the direct piezoelectric effect. The piezoelectric coefficients can be defined as follows:

$$d_{ij} = \left(\frac{\partial D_i}{\partial T_j}\right)^E = \left(\frac{\partial S_i}{\partial E_j}\right)^T; \quad e_{ij} = \left(\frac{\partial D_i}{\partial S_j}\right)^E = -\left(\frac{\partial T_j}{\partial E_i}\right)^T; \quad g_{ij} = -\left(\frac{\partial E_i}{\partial T_j}\right)^D = \left(\frac{\partial S_j}{\partial D_i}\right)^T; \quad h_{ij} = \left(\frac{\partial E_i}{\partial S_j}\right)^D = -\left(\frac{\partial T_j}{\partial D_i}\right)^S \tag{4}$$

Relationships between electrical and elastic mechanical behavior.

Strain – Charge Form: $$S = s_E T + d^t E; D = d.T + \varepsilon_T E \tag{5}$$

Stress- Charge Form: $T = c_E S - e^t E; D = e.S + \varepsilon_s E$ (6)

Strain-Voltage Form: $S = s_D T + g^t D; E = -g.T + \varepsilon_T^{-1} D$ (7)

Stress – Voltage Form: $T = c_D S - q^t D; E = -q.S + \varepsilon_S^{-1} D$ (8)

The linear relationship between the mechanical and electrical fields in the matrix is provided in Abaqus

$$[d] = \begin{bmatrix} d_{1\,11} & d_{1\,22} & d_{1\,33} & d_{1\,12} & d_{1\,13} & d_{1\,14} \\ d_{2\,11} & d_{2\,22} & d_{2\,33} & d_{2\,12} & d_{2\,13} & d_{2\,14} \\ d_{3\,11} & d_{3\,22} & d_{3\,33} & d_{3\,12} & d_{3\,13} & d_{3\,14} \end{bmatrix} \quad (10)$$

$$[e] = \begin{bmatrix} e_{1\,11} & e_{1\,22} & e_{1\,33} & e_{1\,12} & e_{1\,13} & e_{1\,14} \\ e_{2\,11} & e_{2\,22} & e_{2\,33} & e_{2\,12} & e_{2\,13} & e_{2\,14} \\ e_{3\,11} & e_{3\,22} & e_{3\,33} & e_{3\,12} & e_{3\,13} & e_{3\,14} \end{bmatrix} \quad (11)$$

where d_{123}, d_{213}, d_{311}, d_{322}, *and* d_{333} are provided by the manufacturer. Besides, the constant piezoelectric charge *[e]* is also calculated according to the formula (12).

$$[e] = [d][D] \quad (12)$$

With D_{ijkl} is a fourth-order elastic tensor of the elastic stiffness parameter evaluated at a constant electric field

$$[D] = \begin{bmatrix} D_{1111} & D_{1122} & D_{1133} & 0 & 0 & 0 \\ & D_{2222} & D_{2233} & 0 & 0 & 0 \\ & & D_{3333} & 0 & 0 & 0 \\ & & & D_{1212} & 0 & 0 \\ & \text{symmetric} & & & D_{1313} & 0 \\ & & & & & D_{2323} \end{bmatrix} \quad (13)$$

$$\begin{bmatrix} s_1 \\ s_2 \\ s_3 \\ s_4 \\ s_5 \\ s_6 \end{bmatrix} = \begin{bmatrix} s_{11}^E & s_{12}^E & s_{13}^E & 0 & 0 & 0 \\ s_{21}^E & s_{22}^E & s_{23}^E & 0 & 0 & 0 \\ s_{31}^E & s_{32}^E & s_{33}^E & 0 & 0 & 0 \\ & & & s_{44}^E & 0 & 0 \\ & \text{symmetric} & & & s_{55}^E & 0 \\ & & & & & s_{66}^E = 2(s_{11}^E - s_{12}^E) \end{bmatrix} \begin{bmatrix} T_1 \\ T_2 \\ T_3 \\ T_4 \\ T_5 \\ T_6 \end{bmatrix} + \begin{bmatrix} 0 & 0 & d_{31} \\ 0 & 0 & d_{32} \\ 0 & 0 & d_{33} \\ 0 & d_{24} & 0 \\ d_{15} & 0 & 0 \\ 0 & 0 & 0 \end{bmatrix} \begin{bmatrix} E_1 \\ E_2 \\ E_3 \end{bmatrix} \quad (14)$$

$$\begin{bmatrix} D_1 \\ D_2 \\ D_3 \end{bmatrix} = \begin{bmatrix} 0 & 0 & 0 & 0 & d_{15} & 0 \\ 0 & 0 & 0 & d_{24} & 0 & 0 \\ d_{31} & d_{32} & d_{33} & 0 & 0 & 0 \end{bmatrix} \begin{bmatrix} T_1 \\ T_2 \\ T_3 \\ T_4 \\ T_5 \\ T_6 \end{bmatrix} + \begin{bmatrix} \varepsilon_{11} & 0 & 0 \\ 0 & \varepsilon_{22} & 0 \\ 0 & 0 & \varepsilon_{33} \end{bmatrix} \begin{bmatrix} E_1 \\ E_2 \\ E_3 \end{bmatrix} \quad (15)$$

III. NUMERICAL SIMULATION ANALYSIS

Meshing and element type selection greatly influence the numerical simulation results. Finite element models with small mesh sizes will give accurate results. In particular, ultrasonic vibration devices work at very high frequencies while the amplitude is tiny. However, using a mesh size that is too small will increase the number of elements in the model, leading to a very long calculation time. The finite element model of the transducer, used in this study, was created in Abaqus software as shown in Figure 2. The model uses C3D20 elements for conventional material parts, and C3D20RE for ceramic material. PZT8 ceramic material parameters, calculated according to the theoretical basis above, the results obtained are as shown in Table 3 and Table 4.

A series of numerical simulations, corresponding to model mesh sizes of 1 mm, 1.5 mm, 2 mm, 2.5 mm, and 3 mm, respectively, were performed to determine the effect of mesh size on vibration amplitude vibration and

resonant frequency of the ultrasonic transducer. The results obtained are shown in Figure 3 (in case the mesh size is 1.5 mm) and Table 5. From Table 5, it can be seen that the smaller the mesh size, the more accurate the amplitude and resonance frequency values are. However, it is necessary to choose the mesh size to match accuracy and calculation time. Compared with the theoretical values of resonance frequency and amplitude, it is reasonable to choose a mesh size of 1.5 mm for the transducer used in this study. Resonance frequency error is 1.2%, vibration amplitude is 9.7%.

Table 3: **Piezoelectric elastic properties of material**

D_{1111}	D_{1122}	D_{1133}	D_{2233}	D_{3333}
9.02E+10	-5.75E+09	2.18E+10	2.18E+10	8.09E+10
D_{1212}	D_{1313}	D_{2323}	D_{2222}	
4.15E+10	4.15E+10	4.15E+10	9.84E+10	

Table 4: Charge constants matrix in the strain of material

$d_{1\ 11}$	$d_{1\ 22}$	$d_{1\ 33}$	$d_{1\ 12}$	$d_{1\ 13}$	$d_{1\ 23}$	$d_{2\ 11}$	$d_{2\ 22}$	$d_{2\ 33}$
0.0E+00	0.0E+00	0.0E+00	0.0E+00	0.0E+00	3.25E-10	0.0E+00	0.0E+00	0.0E+00
$d_{2\ 12}$	$d_{2\ 13}$	$d_{2\ 23}$	$d_{3\ 11}$	$d_{3\ 22}$	$d_{3\ 33}$	$d_{3\ 12}$	$d_{3\ 13}$	$d_{3\ 23}$
0.0E+00	3.25E-10	0.0E+00	-9.1E-11	-9.1E-11	2.41E-10	0.0E+00	0.0E+00	0.0E+00

Table 5: Piezoelectric charge of material

$e_{1\ 11}$	$e_{1\ 22}$	$e_{1\ 33}$	$e_{1\ 12}$	$e_{1\ 13}$	$e_{1\ 23}$	$e_{2\ 11}$	$e_{2\ 22}$	$e_{2\ 33}$
0.0E+00	0.0E+00	0.0E+00	0.0E+00	0.0E+00	1.37E+01	0.0E+00	0.0E+00	0.0E+00
$e_{2\ 12}$	$e_{2\ 13}$	$e_{2\ 23}$	$e_{3\ 11}$	$e_{3\ 22}$	$e_{3\ 33}$	$e_{3\ 12}$	$e_{3\ 13}$	$e_{3\ 23}$
0.0E+00	1.37e+01	0.0E+00	-1.87E+00	-1.87E+00	1.370E+01	0.0E+00	0.0E+00	0.0E+00

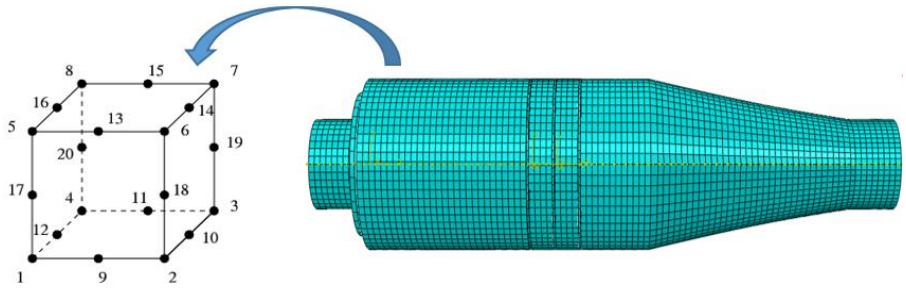

Figure 2: Finite element model of transducer

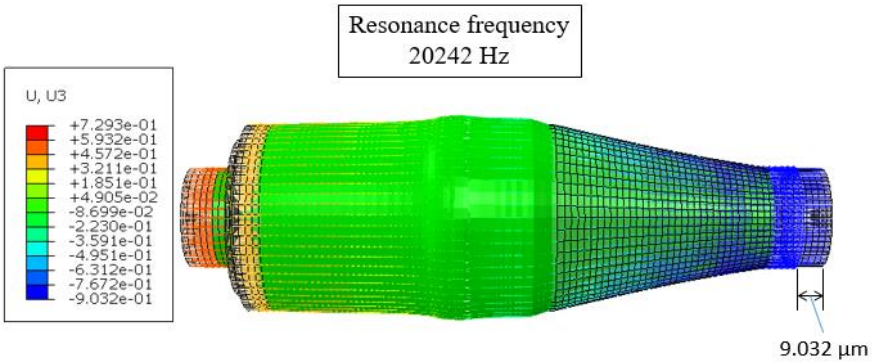

Figure 3: Vibration amplitude of the ultrasonic transducer

Table 6: Comparison of simulation results for different mesh sizes

Mesh size (mm)	Resonance frequency (Hz)	Vibration amplitude (µm)	Time CPU (s)
1	19986	9.45	2728
1.5	20242	9.03	1799
2	21983	8.76	1382
2.5	23278	8.45	978
3	25378	7.87	563

IV. CONCLUSION

In this study, the influence of mesh size on the longitudinal vibration amplitude of the transducer was studied through numerical simulations for models with many different mesh sizes. The results show that the vibration amplitude is very sensitive to changing the mesh size. The results of this study can be used as a basis to research and evaluate the influence of mesh size in the complete model of an ultrasonic vibration system.

REFERENCES

[1] S. Yadav and C. Doumanidis (2005), "Thermomechanical analysis of an Ultrasonic Rapid Manufacturing (URM) system," J. Manuf. Process., vol. 7, no. 2, pp. 153–161

[2] Y. Daud, M. Lucas, and Z. Y. Huang (2006), "Ultrasonic Compression Tests on Aluminium," pp. 99–104.

[3] Y. Daud, M. Lucas, and Z. Huang (2007), "Modelling the effects of superimposed ultrasonic vibrations on tension and compression tests of aluminium," J. Mater. Process. Technol., vol. 186, no. 1–3, pp. 179–190.

[4] M. Inoue (1984), "Studies on ultrasonic metal tube drawing," Sagami, Mem. Inst. Technol., vol. 19, pp. 1–7.

[5] L. B (1961), "Work-softening of metal crystals by alternating the rate of glide strain," Acta Metall., vol. 9, no. 10, pp. 937–940.

[6] J. A. Gallego-Juárez, G. Rodriguez, V. Acosta, and E. Riera (2010), "Power ultrasonic transducers with extensive radiators for industrial processing," Ultrason. Sonochem., vol. 17, no. 6, pp. 953–964.

[7] M. C. W. Wu X, Liu T (2017), "welding mechanism, and failure of Al/Cu ultrasonic welds," Ultrason. Weld. Lithium-Ion Batter., pp. 37–54.

[8] M. P. Satpathy and S. K. Sahoo (2016), "Microstructural and mechanical performance of ultrasonic spot welded Al-Cu joints for various surface conditions," J. Manuf. Process., vol. 22, pp. 108–114.

[9] V. Kumar (2011), "Understanding ultrasonic plastic assembly,"

[10] D. A. DeAngelis, G. W. Schulze, and K. S. Wong (2015), "Optimizing Piezoelectric Stack Preload Bolts in Ultrasonic Transducers," Phys. Procedia, vol. 63, pp. 11–20.

[11] K. Ngo-Nhu et al.(2023), "A new algorithm to calculate complex material parameters in piezoelectric stacks," Lat. Am. J. Solids Struct., vol. 20, no. 3.

[12] V. D. Luong, P. T. M. Duong, T. B. N. Nguyen, N. K. Ngo, T. H. Nguyen, and V. Du Nguyen (2023), "Dynamic Response of High-Power Ultrasonic System Based on Finite Element Modeling of Piezoelectric," J. Appl. Eng. Sci., vol. 21, no. 3, pp. 859–871, .

[13] B. Chandra Behera, "Development and Experimental Study of Machining Parameters in Ultrasonic Vibration-assisted Turning," 2011. [Online]. Available: http://ethesis.nitrkl.ac.in/4416/1/Development_and_experimental_study_of_machining_parameters_in_ultrasonic_vibration-assisted_turning.pdf

[14] A. C. Mathieson (2012), "Nonlinear Characterisation Of Power Ultrasonic Devices Used In Bone Surgery," [Online]. Available: http://theses.gla.ac.uk/3135/

[15] X. Li, P. Harkness, K. Worrall, R. Timoney, and M. Lucas (2017), "A Parametric Study for the Design of an Optimized Ultrasonic Percussive Planetary Drill Tool," IEEE Trans. Ultrason. Ferroelectr. Freq. Control, vol. 64, no. 3, pp. 577–589.